



OPEN ACCESS

EDITED BY

Thomas Beyer,
Medical University of Vienna, Austria

REVIEWED BY

Paul Cumming,
University of Bern, Switzerland
Miho Shidahara,
Tohoku University, Japan

*CORRESPONDENCE

Supatporn Tepmongkol,
✉ supatporn.t@chula.ac.th

RECEIVED 01 June 2023

ACCEPTED 25 September 2023

PUBLISHED 10 October 2023

CITATION

Khamwan K, Sukprakun C, Limotai C, Jirasakuldej S, Jantarato A, Hemachudha T and Tepmongkol S (2023), Dynamic ^{18}F -FDG-PET kinetic parameters for epileptogenic zone localization in drug-resistant epilepsy. *Front. Phys.* 11:1233059. doi: 10.3389/fphy.2023.1233059

COPYRIGHT

© 2023 Khamwan, Sukprakun, Limotai, Jirasakuldej, Jantarato, Hemachudha and Tepmongkol. This is an open-access article distributed under the terms of the [Creative Commons Attribution License \(CC BY\)](https://creativecommons.org/licenses/by/4.0/). The use, distribution or reproduction in other forums is permitted, provided the original author(s) and the copyright owner(s) are credited and that the original publication in this journal is cited, in accordance with accepted academic practice. No use, distribution or reproduction is permitted which does not comply with these terms.

Dynamic ^{18}F -FDG-PET kinetic parameters for epileptogenic zone localization in drug-resistant epilepsy

Kitiwat Khamwan^{1,2}, Chanan Sukprakun¹, Chusak Limotai^{3,4}, Suda Jirasakuldej^{3,4}, Attapon Jantarato⁵, Thiravat Hemachudha⁶ and Supatporn Tepmongkol^{1,2,4,7*}

¹Division of Nuclear Medicine, Department of Radiology, Faculty of Medicine, Chulalongkorn University, Bangkok, Thailand, ²Chulalongkorn University Biomedical Imaging Group, Department of Radiology, Faculty of Medicine, Chulalongkorn University, Bangkok, Thailand, ³Department of Medicine, Faculty of Medicine, Chulalongkorn University, Bangkok, Thailand, ⁴Chulalongkorn Comprehensive Epilepsy Center of Excellence (CCEC), King Chulalongkorn Memorial Hospital, Bangkok, Thailand, ⁵National Cyclotron and PET Centre, Chulabhorn Hospital, Chulabhorn Royal Academy, Bangkok, Thailand, ⁶Department of Medicine (Neurology), Neuroscience Centre for Research and Development, Thai Red Cross Emerging Infectious Disease-Health Science Centre, Faculty of Medicine, Chulalongkorn University, Bangkok, Thailand, ⁷Cognitive Impairment and Dementia Research Unit, Faculty of Medicine, Chulalongkorn University, Bangkok, Thailand

Objective: Precisely localizing the seizure onset zone remains a challenging task in drug-resistant epilepsy (DRE) patients especially given its critical role in successful surgery and effective management. This study aimed to investigate the kinetic parameters of regional ^{18}F -fluorodeoxyglucose (FDG) uptake in DRE patients, aiming to identify the kinetic parameters best enabling the identification of the epileptogenic region.

Methods: Consecutive DRE patients with clinically mandated interictal ^{18}F -FDG PET/CT were recruited from October 2019 to September 2020 for pre-surgical evaluation. Immediately after injecting ^{18}F -FDG of 112–179 MBq, dynamic data were acquired for 90 min. The motion correction and resampling to the Montreal atlas was performed in order to generate a transformation matrix. 116 volume of interests (VOIs) and regional time-activity curves (TACs) were generated by employing the automated anatomical labeling (AAL) template using PMOD software. Kinetic parameters of FDG unidirectional blood-brain clearance (K_1), efflux (k_2), phosphorylation (k_3), and net metabolic flux (K_i) were derived using irreversible 2-tissue-compartment model with an image-derived input function (IDIF). The kinetic parameters values obtained from all regions were ranked and compared with the presumed epileptogenic zone (EZ).

Results: Eleven DRE patients (5 males, 6 females, mean age 35.1 ± 10.2 years) were analyzed. We found that the region with the lowest values of K_i provided correct lateralization in 7/7 (100%) of patient with temporal lobe epilepsy (TLE) and the region with the lowest K_i and k_3 parameters showed concordance with the EZ in 100% and 71.4% of patients, respectively.

Conclusion: The present parametric approach to the evaluation of FDG-PET may be more sensitive than semi-quantitative approaches for the detection of

pathophysiology in the EZ of patients with medically unresponsive TLE in addition to the routine clinical investigations.

KEYWORDS

drug-resistant epilepsy, pharmacokinetic modeling, compartmental modeling, dynamic-PET, PMOD software, epileptogenic zone localization

1 Introduction

Epilepsy is a prevalent neurological disorder that affects millions worldwide, and about one-third of patients with epilepsy become medically intractable, often requiring surgery for achievable management [1]. Precisely localizing the epileptogenic zone (EZ) is essential for successful surgical intervention. Functional imaging techniques such as ^{99m}Tc -ethyl cysteinate dimer (ECD) ictal-interictal single photon emission computed tomography (SPECT) and ^{18}F -fluorodeoxyglucose-positron emission tomography (FDG-PET) play a crucial role in identifying EZ and differentiating them from non-epileptogenic regions, particularly in patients with drug-resistant epilepsy (DRE) or discordant cases where conventional magnetic resonance imaging (MRI) has limited sensitivity [2–5]. ^{18}F -FDG PET is typically used in interictal studies for presurgical evaluation since ictal studies are difficult to obtain due to slow brain glucose uptake and the short decomposition time of ^{18}F . The main advantage of interictal ^{18}F -FDG PET over interictal ^{99m}Tc -ECD SPECT is that ^{18}F -FDG PET provides a better spatial resolution, thus results in higher diagnostic sensitivity for EZ localization [6].

In epilepsy, it was known that there is mutation of gene controlling oxidative phosphorylation affecting mitochondrial function [7–11]. Since the structure of mitochondria is disrupted in neuropathological study, the utilization of glucose in this area is less. This results in the focally reduced FDG uptake or the known relative hypometabolism in the EZ. However, the limitations of static FDG-PET (sFDG-PET) in accurately defining the surgical margin pose a significant challenge [12, 13]. Overcoming these limitations and achieving accurate localization of the seizure origin remain the greatest challenges for epilepsy pre-surgical evaluation.

Pharmacokinetic (PK) modeling plays a critical role in studying radiotracer kinetics in the human body, particularly in the field of nuclear medicine, which includes neuroimaging [14–16]. Applying kinetic models and quantifying PET data is of great interest for accurately localizing seizure onset zones in difficult epilepsy cases. While some studies have shed light on local cerebral FDG metabolism during epilepsy, our understanding of this phenomenon is limited, and most previous studies have investigated FDG kinetics in healthy adults or animals [17–22]. Their applicability to epilepsy has yet to be ascertained. As such, the establishment of PK models specific to epilepsy is a critical need, and would help optimize treatment for patients with DRE.

To achieve accurate localization of EZ, it is crucial to understand the differences in FDG kinetics and transfer rate between EZ and normal human brain areas. Therefore, the present study aimed to investigate the kinetic parameters for regional FDG uptake in DRE patients utilizing interictal dynamic FDG-PET (dFDG-PET) PK models. Quantitative analysis in terms of PK models that provide transfer rates and quantification in each region of the brain derived

in this study can improve the localization of EZ for intractable epilepsy, ultimately leading to better management and outcomes for patients.

2 Materials and methods

2.1 Subjects

This study was conducted in accordance with the guidelines and regulations of our institutional review board (IRB) and obtained approval prior to patient recruitment. Consecutive DRE patients who underwent a prolonged video-electroencephalography (EEG) monitoring for presurgical evaluation and required ^{18}F -FDG PET/CT study during October 2019 to September 2020 were scanned in this study. Written informed consent was obtained from all patients prior to the examination. Patients were received anti-seizure medications as per their usual regimen at the time of scanning procedure in order to control the seizure condition. All patients underwent MRI brain epilepsy protocol with T1-weighted and T2-weighted sequences. Patients who had last seizure within 48 h prior to the examination, or lacked EEG data were excluded from the study.

2.2 Dynamic PET/CT image acquisition

To conduct the kinetic modeling, PET/CT imaging was performed using a Siemens Biograph Vision 64-slice digital PET/CT system. All patients fasted for at least 6 h before the study. Prior to injection, blood glucose levels were checked to ensure the level below 120 mg/dL. Each patient was intravenously injected with 2.6 MBq/kg of ^{18}F -FDG (half-dose protocol) and immediately followed by a 90-min dynamic PET scan. List-mode data were acquired and binned into 31 frames: 6×10 s, 8×30 s, and 17×300 s. PET image series for each frame was reconstructed using time-of-flight ordered subset expectation maximization (OSEM) algorithm with 8 iterations and 5 subsets, and matrix size of 440×440 . Corrections for radioactivity decay, attenuation, model-based scatter, random events, and 5 mm Gaussian filtering of convolution kernel were applied to all PET image reconstructions. A low-dose CT scan protocol was used for attenuation correction and localization.

In this study, a non-invasive method, image-derived input function (IDIF) was utilized for alternative invasive arterial blood sampling [13, 23, 24]. The regions of interest (ROIs) were drawn by iso-contour (3D iso-contouring VOI tools using region-growing) inside the right internal carotid artery (ICA) in order to generate time-activity curve (TAC) input function for the kinetic modeling. Figure 1 shows the dFDG-PET images varying over time, which were used for generating the TAC at the internal carotid artery region as a non-invasive input function.

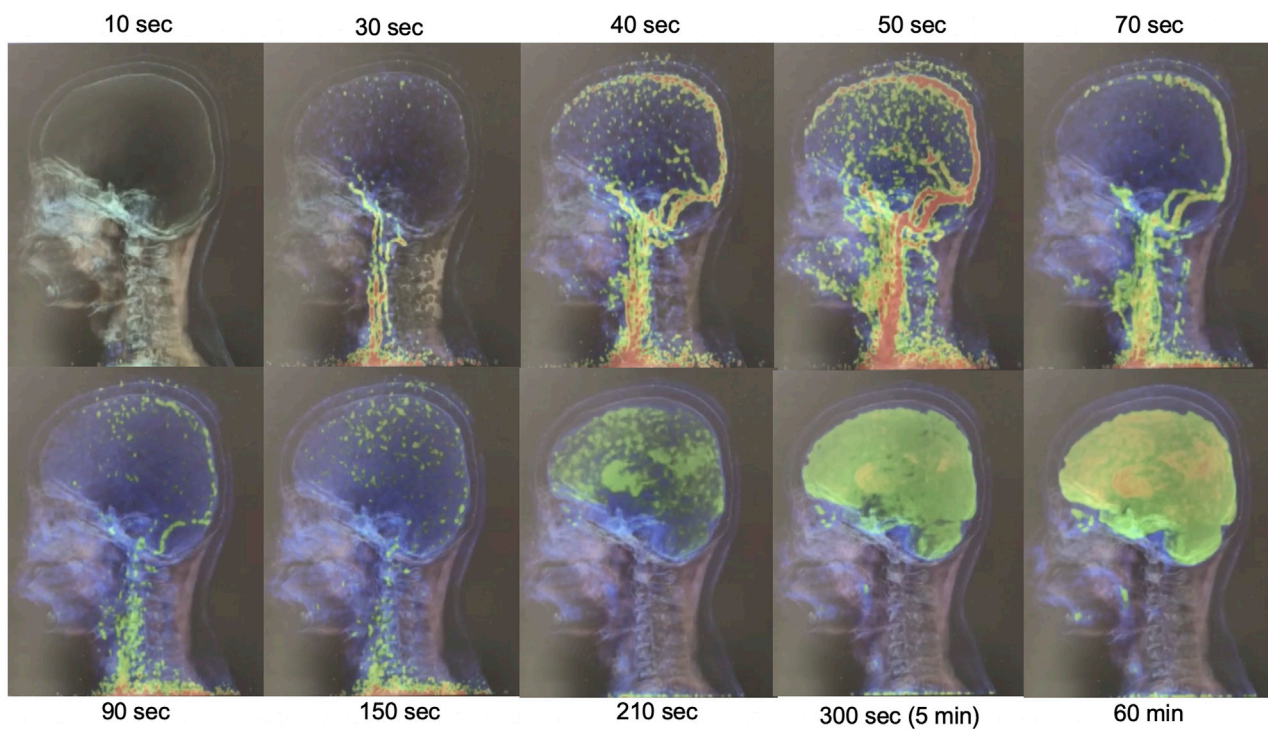
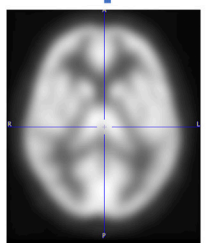
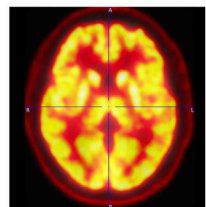


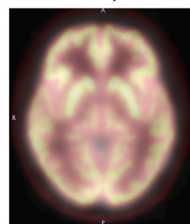
FIGURE 1
Illustration of dynamic-FDG PET images changing over-time for measuring the input function at the internal carotid artery region.

dFDG-PET in native space after motion correction

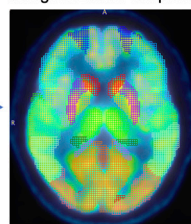


Template PET in MNI space

Coregistered PET in MNI space



Pre-defined VOIs in MNI space using AAL atlas template



Generate 116 regional TACs

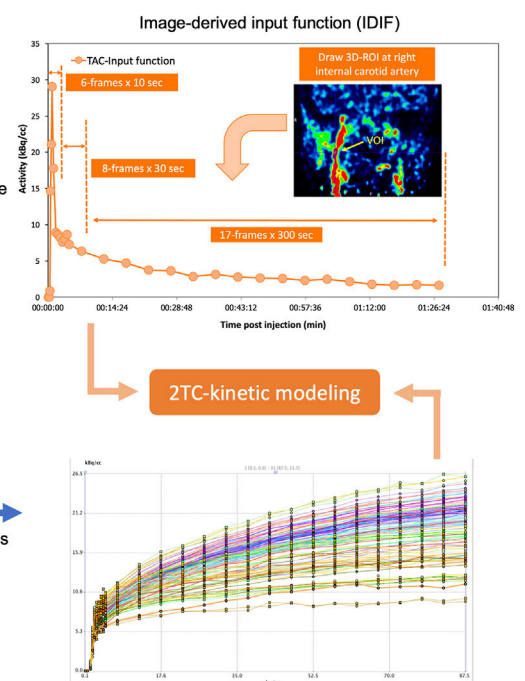


FIGURE 2
Overall workflow for PK model based on 2-tissue compartment (2TC) utilizing image-derived input function measured from dFDG-PET.

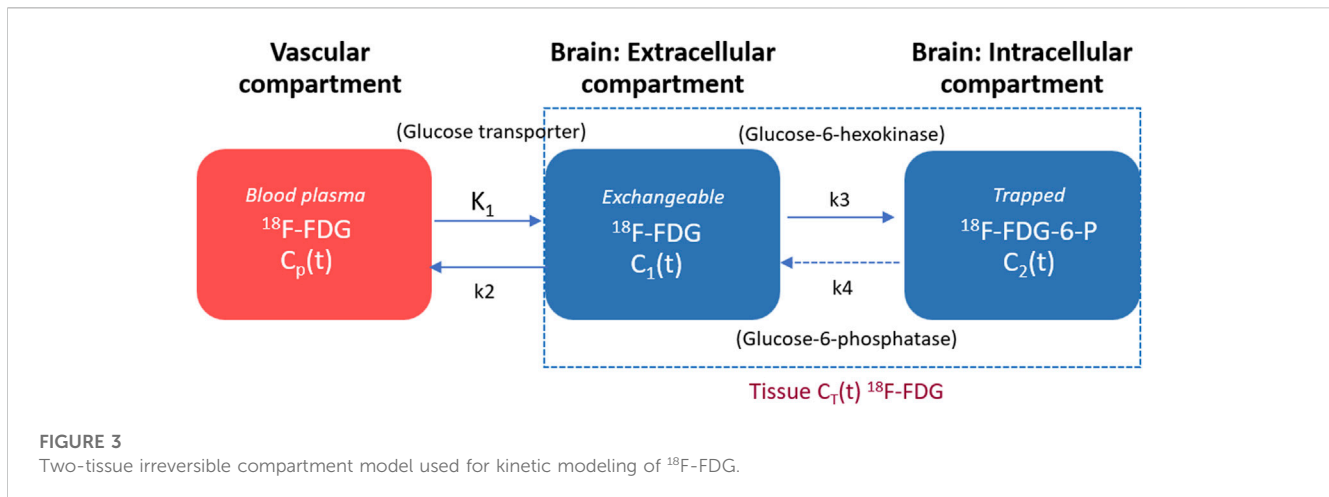


FIGURE 3
Two-tissue irreversible compartment model used for kinetic modeling of ¹⁸F-FDG.

2.3 Regional tissue time-activity curves

In this study, 31 time-frames of dynamic PET images were transferred to the PMOD software (PMOD 4.101, PMOD Technologies Ltd.) to determine the FDG kinetic parameters in each patient. Image pre-processing was initiated with motion correction for the 90-min acquisition for the deformation process. PET data were averaged across the early 5 time-frames series to create a reference, which was used to perform a rigid body transform across all 31 frames of the dynamic PET. The motion-corrected PET frames were then re-sliced and co-registered with a PET template in the Montreal Neurological Institute (MNI) space using a non-rigid transform to generate a transformation matrix. The transformation information was then used to reorient the dynamic image into the MNI space. The resulting transformation matrix was inverted and applied to all ROIs to move them from the standard MNI template into the patient PET. A set of predefined volume of interests (VOIs) utilizing an automated anatomical labeling (AAL) template atlas was used to generate 58 VOIs per hemisphere, creating a total of 116 regional TACs for calculating the kinetic parameters. The overview workflow for spatial normalization, AAL atlas, which was used to automatically extract the VOIs and TACs for 116 local brain regions, and the IDIF for PK model, which was obtained using dynamic PET scan, is illustrated in Figure 2.

2.4 Compartmental modeling

By employing dFDG-PET measurements, the irreversible two-tissue compartment (2TC) model was used to develop the kinetic modeling for the dFDG-PET data utilizing the PKIN kinetic modeling module. The compartmental model used to describe the behaviors of FDG in brain tissue is depicted in Figure 3. The left compartment represents the vascular space for FDG, the center compartment represents the tissue space for free FDG, and the right compartment represents the tissue space for ¹⁸F-FDG-6-phosphate (FDG-6-P). The transfer rate constants between compartmental tissues are represented by K_1 (FDG unidirectional blood-brain

clearance), k_2 (efflux), and k_3 (phosphorylation). The corresponding ordinary differential equation of 2TC FDG kinetic modeling of each compartment can be expressed using Eq. 1 as follows [25, 26]:

$$\frac{d}{dt} \begin{bmatrix} C_1(t) \\ C_2(t) \end{bmatrix} = \begin{bmatrix} -(k_2 + k_3) & 0 \\ k_3 & 0 \end{bmatrix} \begin{bmatrix} C_1(t) \\ C_2(t) \end{bmatrix} + \begin{bmatrix} K_1 \\ k_4 = 0 \end{bmatrix} C_{wb}(t), \quad (1)$$

where $C_{wb}(t)$ represents the ¹⁸F-FDG activity concentration in whole blood derived from IDIF, $C_1(t)$ represents the activity concentration of free ¹⁸F-FDG, and $C_2(t)$ represents the activity concentration of metabolized or trapped ¹⁸F-FDG in the tissue space at time t . The constant K_1 (unit: mL/min/cm³) is the rate of ¹⁸F-FDG delivery from the whole blood to the tissue space, k_2 (unit: min⁻¹) is the rate constant of tracer leaving the tissue space, whereas k_3 (unit: min⁻¹) is the rate constant of ¹⁸F-FDG being phosphorylated by hexokinase. Typically, this irreversible model widely assumes that the dephosphorylation process is negligible, therefore, FDG k_4 rate constant can be considered to be zero (i.e., $k_4 = 0$) for the majority of tissues. As a result, the irreversible FDG model using PMOD in this study includes 3 fittable parameters (i.e., K_1 , k_2 , k_3). With regard to non-linear fitting of kinetic parameters, the initial values of K_1 , K_1 , k_2 , and k_3 were set to 0.05, 0.1, 0.01, and 0.01, respectively. The lower bound and the upper bound were set from zero to eight for all mentioned parameters.

The macro parameter K_i representing the net metabolic influx rate of ¹⁸F-FDG consumption can be calculated using Eq. 2 as follows [26, 27]:

$$K_i = \frac{K_1 k_3}{k_2 + k_3} \quad (2)$$

The total radioactivity concentration in the tissue compartment as a function of time ($C_{PET}(t)$) that can be measured by PET is the sum of the time courses of ¹⁸F-FDG in the vascular, intravascular and extravascular spaces, which can be written using Eq. 3 as follows [25–27]:

$$C_{PET}(t) = C_{wb}(t) \otimes \left(\frac{K_1 k_2}{k_2 + k_3} e^{-(k_2 + k_3)t} + \frac{K_1 k_3}{k_2 + k_3} \right), \quad (3)$$

TABLE 1 Patient demographics data.

Id	Age/ Sex	Injected activity (MBq)	Blood glucose level (mg/dL)	Clinical localization/lateralization	EEG location	MRI brain	Interictal PET/CT
1	26/M	150	91	Rt. temporal	Rt. mesial temporal	Probably right hippocampal sclerosis	Hypometabolism at antero-lateral right temporal lobe
2	47/F	125	77	Lt. temporal	Intermittent slow Lt. cerebral hemisphere with Lt. temporal lobe predominance	Left hippocampal sclerosis	Hypometabolism at left medial temporal lobe
3	22/F	140	81	Rt. parietal	IED spike C ₂ P ₂ , C ₄ , ictal EEG: repetitive spike C ₂ C ₄	Relatively small gyri at superior aspect of anterior right temporal lobe	Suspicious of a small area of subtle mild hypometabolism at right inferomedial temporal lobe
4	38/M	125	109	Lt. hemisphere	Rt. temporal (ictal EEG Rt. temporal, IED bilateral R > L)	Left hippocampal sclerosis, Traumatic brain injury Lt. frontal and bilateral superior temporal	Hypometabolic focus at anterior left temporal lobe
5	35/M	110	85	Lt. temporal	Lt. temporal-occipital-parietal	Negative	Suspicious area of functional deficit zone at left temporal lobe (lateral, anterior and mesial)
6	31/F	112	89	Rt. temporal	Ictal EEG 4/4 Rt. (Rt frontal or Rt. Insula), IED—Rt. temporal, Lt. temporal, Lt. frontotemporal	Negative	Bilateral temporal metabolism is quite equal except area of relatively lower at left temporal pole
7	38/M	179	88	Rt. temporal	Ictal EEG: Rt. temporal 3/3, interictal EEG: Rt. temporal	Right occipital cortical-based tumor	Hypometabolism at the whole right temporal cortex
8	19/F	132	79	Rt. hemisphere	Ictal EEG → Rt. temporal-occipital-parietal 2/3 and 1/3 Lt. temporal Interictal EEG → Rt. PTO > Rt. frontal > bilat. occipital (Rt > Lt)	Left frontal focal cortical dysplasia (FCD), ± Right occipital FCD	Relatively hypometabolism at bilateral posterior parietal regions
9	41/F	132	75	Rt. temporal	Ictal EEG → Rt. temporal 8/8, interictal EEG → Rt. & Lt. temporal	Few hyperintense foci without restricted diffusion in right temporal stem. Brain atrophy	No evidence of focal hypometabolism
10	53/F	140	107	Lt. temporal	Lt temporal	Ill-defined internal architecture in posterior left hippocampal body	Hypometabolism at left lateral temporal lobe
11	36/M	145	79	Lt. hemisphere	Ictal EEG → Lt. 4/7, Rt. 3/7, interictal EEG → Lt. temporal, Lt. frontal	Few small non-specific white matter changes	Hypometabolism at the left temporal lobe

where \otimes is the convolution operation symbol, K_1 is the rate of ¹⁸F-FDG entry into the tissue, while $k_3/(k_2+k_3)$ represents how much ¹⁸F-FDG is metabolized or trapped as mentioned previously. For model fitting, the fraction of blood volume (vB, unit: mL/mL) is fixed at a physiologic value of approximately 5% to reduce the number of fitted parameters [15, 18, 19, 26, 28].

2.5 Potential epileptogenic zone verification

The consensus of the area of potential EZ was made by the multidisciplinary epilepsy team which consisted of epileptogists,

neurosurgeons, diagnostic radiologists and nuclear medicine physicians. At the time of this study, results of the kinetic ¹⁸F-FDG study were not as part of information used for consensus decision.

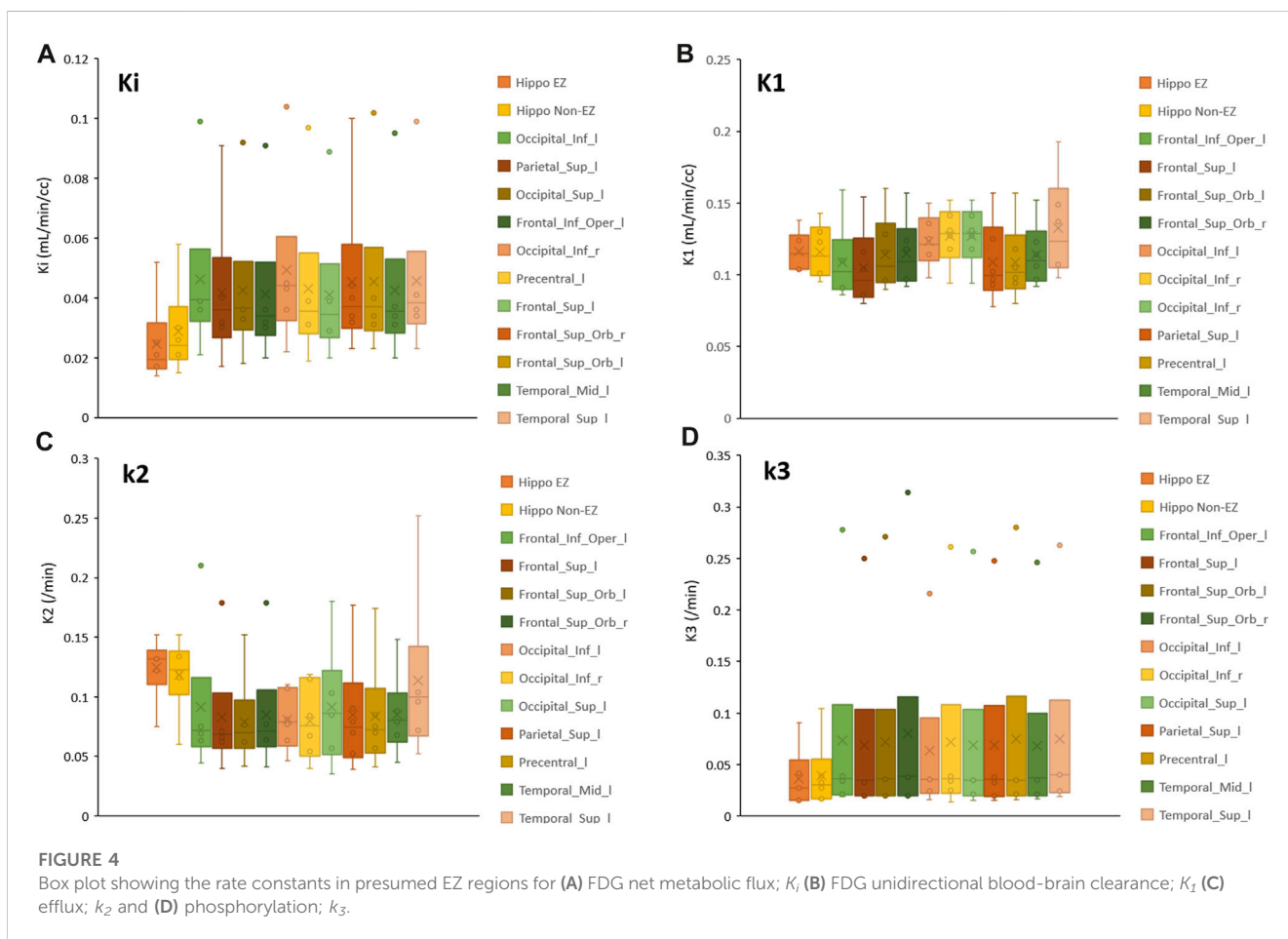
2.6 Data analysis

The kinetic parameters of K_1 , K_1 , k_2 , and k_3 derived from kinetic modeling of 116 regions in each patient were analyzed. All rate constants among these regions were ranked and the lowest value of kinetic parameters was chosen, and compared with the

TABLE 2 Summary of suspected epileptogenic zone by pre-surgical workups and associated kinetic parameter findings.

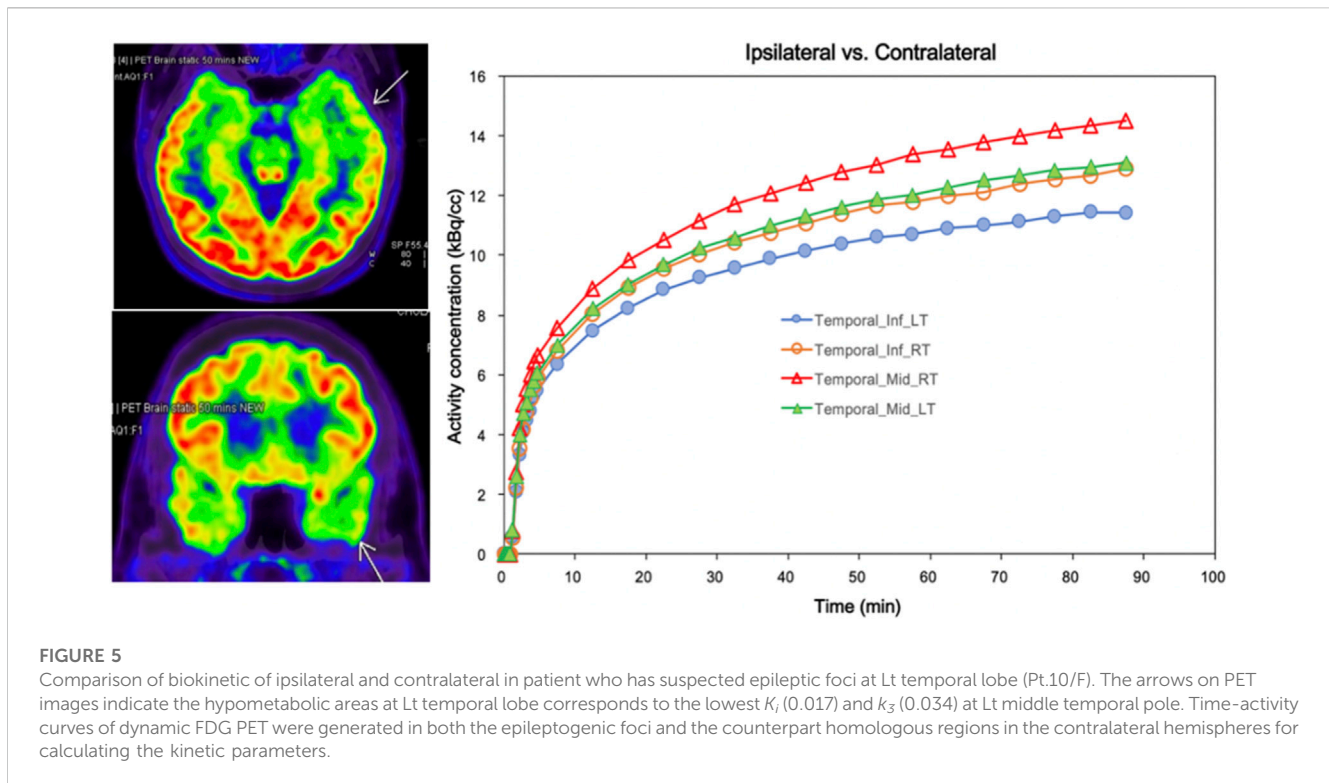
Id	Suspected epileptogenic area		Lowest K_i	Lowest K_1	Lowest k_2	Lowest k_3	Associated kinetic parameter findings
1	Rt. temporal	TLE	Rt. hippo	Temporal_Inf_l	Occipital_Inf_l	Rt. hippo	K_i, k_3
2	Lt. temporal	TLE	Lt. hippo	Parietal_Sup_l	Parietal_Sup_l	Lt. hippo	K_i, k_3
3	Inconclusive	-	Rt. hippo	Frontal_Inf_Oper_l	Frontal_Inf_Oper_l	Frontal_Sup_Orb_l	n/a
4	Lt. temporal	TLE	Lt. hippo	Frontal_Sup_l	Occipital_Sup_l	Lt. hippo	K_i, k_3
5	Lt. temporal	TLE	Lt. hippo	Parietal_Sup_l	Occipital_Inf_r	Occipital_Sup_r	K_i
6	Inconclusive	-	Temporal_Pole_Sup_l	Frontal_Sup_r	Precentral_l	Lt. hippo	n/a
7	Rt. temporal	TLE	Rt. hippo	Temporal_Inf_l	Frontal_Sup_l	Rt. hippo	K_i, k_3
8	Inconclusive	-	Rt. hippo	Rt. hippo	Frontal_Sup_Orb_r	Rt. hippo	n/a
9	Rt. temporal	TLE	Rt. hippo	Temporal_Pole_Mid_r	Frontal_Sup_Orb_l	Temporal_Pole_Mid_l	K_i
10	Lt. temporal	TLE	Temporal_Pole_Mid_l	Temporal_Pole_Mid_l	Temporal_Pole_Mid_l	Temporal_Pole_Mid_l	K_i, k_1, k_2, k_3
11	Inconclusive	-	Parietal_Sup_r	Temporal_Pole_Sup_l	Temporal_Pole_Sup_l	Lt. hippo	n/a

Tem, temporal; TLE, temporal lobe epilepsy; Hippo, hippocampus; Sup, superior; Mid, middle; Inf, inferior; n/a, unable to associate kinetic parameter with the epileptogenic zone due to inconclusive epileptogenic area.



presumed EZ identified by the concordance of at least 3 out of 4 pre-surgical workups, which are clinical semiology, scalp EEG, MRI, and static FDG-PET visual analysis results. The presumed

EZ as established through the previously mentioned concordance was determined by assigning it to a specific region based on the AAL atlas.



3 Results

Eleven patients with DRE, aged 19–53 years (5 males, 6 females, mean age 35.1 ± 10.2 years) were carried out. Table 1 presents the characteristics of the study subjects with DRE referred to dFDG-PET in this study. The mean ^{18}F -FDG activity administered to the patients was 135.5 ± 19.2 MBq, ranging from 110–179 MBq, and all dynamic scans of the 11 DRE patients were successful. Negative MRI findings were found in 2 patients (patient 5 and patient 6). Table 2 lists the summary of suspected area of EZ and related kinetic parameter findings. In this study, the suspected areas for EZ were found at the left temporal lobe in 4 patients, right temporal lobe in 3 patients, and inconclusive in 4 patients (patients 3, 6, 8, and 11). We thus excluded the patients who had inconclusive EZ due to the discordance of clinical, EEG, MRI, and PET/CT interpretation from the analysis of this study. When the lowest value of kinetic parameters was chosen and compared with the presumed EZ, we found that the net metabolic flux K_i and the rate constant k_3 kinetic parameters provided high association with the suspected EZ in all patients. The lowest K_i values were concordance with the suspected EZ in all the remaining EZ identifiable 7 patients, while the lowest k_3 values were found concordance in 5 out of 7 patients (71.7%).

Figure 4 illustrates the box plots of the rate constants of K_i , K_1 , k_2 and k_3 in presumed EZ regions found in this study. The plots indicated that the values of K_i and k_2 were significantly lower and higher, respectively, in the presumed EZ regions compared to other regions. The details of regional FDG kinetic parameters determined from 11 DRE patients are provided in Supplementary Material S1.

Figure 5 illustrates a comparison of the biokinetic in the presumed EZ and homologous regions in the contralateral hemisphere of a patient suspected to have presumed EZ in the

left temporal region, showing hypometabolic areas at the left temporal lobe. The kinetic parameters were calculated from TAC generated from both the epileptogenic foci and counterpart homologous regions in the contralateral hemispheres. The lowest K_i values of $0.017 \text{ mL/min/cm}^3$ and k_3 of 0.034 min^{-1} were found in the left middle temporal pole region for this case, which were associated with the clinical diagnosis and EEG location.

4 Discussion

Improving the localization of epileptic foci in DRE is of great interest, as visualization of hypometabolic areas on FDG-PET is non-specific to the EZ [29, 30]. In recent years, there have been huge efforts in using nuclear medicine techniques, both by visual and by quantitative analysis, for better localizing EZ [30]. Among these, the study of FDG biokinetic pattern in epilepsy is a method that has potential to benefit patients in clinical settings by avoiding invasive diagnoses [13]. To address this, we further investigated the kinetic parameters of regional FDG uptake using a 2TC-PK model of dFDG-PET in DRE patients for pre-surgical evaluation to see if a single kinetic parameter or a combination would benefit in EZ localization or not. Based on our results, we found that the lowest net metabolic flux (K_i) values were concordance with all of the presumed EZ. In addition, the rate constant of ^{18}F -FDG phosphorylation (k_3) was also lowest in 5 of 7 patients. Thus, both of these kinetic parameters can be used in isolation without comparison to any other brain reference regions (e.g., contralateral homologous brain region, cerebellum, pons, etc.). Of note is that although some patients showed that there were other structural abnormalities on their MRI (patients 4 and 9) or even if there was a lesion not related

to epileptogenicity (patient 7), the lowest K_i and k_3 were still located at the epileptogenic region. So, the utilization of dFDG-PET imaging combined with pharmacokinetic modeling has a potential to provide important information for the assessment and characterization of epileptic foci in DRE patients with discordant pre-surgical investigation data in addition to the use of FDG-PET visual analysis alone.

According to distribution of the kinetic values in representative brain regions illustrated in Figure 4, we observed that K_i and k_3 showed decreasing trends, while k_2 showed higher values in the presumed EZ. We also found that K_i was the lowest in all seven EZs, k_3 was the lowest in 5 out of 7 patients, and k_2 was the highest in 4 out of 7 patients. According to these results, we suggested that k_3 's low value and high k_2 might contribute to the low K_i . The high k_2 values could be due to the accumulation of radiotracer in the extracellular compartment in the EZ, resulting in a high flux of the radiotracer back into the bloodstream.

Reference [18] described a mathematical model based on blood sampling to determine a local cerebral metabolic rate of glucose in 13 healthy subjects. The average kinetic parameters of FDG (K_i , K_1 , k_2 and k_3) in gray matter were 0.0334 ± 0.0058 , 0.102 ± 0.028 , 0.130 ± 0.066 , and $0.062 \pm 0.019 \text{ min}^{-1}$ respectively, while in white matter were 0.0154 ± 0.0035 , 0.054 ± 0.014 , 0.109 ± 0.044 , and $0.045 \pm 0.019 \text{ min}^{-1}$ respectively. Although the kinetic parameters K_i , K_1 , k_2 and k_3 in the suspected EZ of our study, as depicted in Figure 4, closely matched those reported by Huang et al, there were notable exceptions in the hippocampus areas for both EZ and non-EZ regions. It is important to note that Huang et al. reported their kinetic parameters in gray matter and white matter regions. Consequently, direct comparisons between their findings and those of our study may not be comparable, as we have reported the kinetic parameters specific to each local region derived from the AAL atlas.

In comparison to our study, Ref. [13] assessed the use of asymmetry indexes (ASYM) derived from dFDG-PET and from static FDG PET to identify the pathophysiology of metabolism in intractable epilepsy. They found that hypometabolism within epileptic foci may be related to reduced glucose phosphorylation (k_3) compared to capillary influx (K_i). This is in line with our study, in which k_3 was usually lowest in the presumed EZ. This was also proven in a study of patients with temporal lobe epilepsy, in which the oxidative metabolism of glucose was reduced in the area of epileptogenicity, not the decrease of neuronal density [31]. The lowest net flux (K_i) in our study may be the result of low k_3 as it is frequently the lowest parameter in the EZ. This finding corresponds with the previous genetic and pathological studies mentioned earlier in the introduction that the affecting pathology in epilepsy focused on phosphorylation, aka hexokinase activity or k_3 in kinetic modeling. However, there might also be other factors causing low K_i because some of the presumed EZ did not show lowest k_3 value.

The study by Ref. [12] utilized the parametric quantification from dFDG-PET imaging to locate hypometabolic foci in patients with no MRI evidence of focal epilepsy. The lowest negative z-scores were identified as hypometabolic. Their study found that dFDG-PET was able to detect focal regions of altered metabolism in all cases where standard clinical FDG-PET found no abnormalities. However, the authors suggest that further study is warranted to evaluate the specificity and sensitivity of dFDG-PET in larger

cohorts to determine whether glucose dynamics can improve clinical utility for localization of epileptic foci over standard static PET techniques.

The reduced interictal uptake of ^{18}F -FDG in the temporal lobe ipsilateral to the seizure focus in temporal lobe epilepsy (TLE) patients was studied by Ref. [32]. They attributed this reduction to regional differences in the lumped constant (λ), indicative of altered glucose metabolism. Our study aligns with this finding by demonstrating altered glucose metabolism in DRE patients, emphasizing the importance of accurate metabolic assessments for epilepsy evaluation. The study by Ref. [33] focused on the coupling between regional cerebral glucose metabolism (rCMRGlc) and blood flow (rCBF) in TLE patients. They found a mismatch between metabolism and blood flow in the temporomesial structures, indicating that alterations in glucose metabolism might not always correspond to changes in blood flow. Their study resonates with our findings, as we observed a specific kinetic parameter, the K_i and k_3 to be a more reliable indicator of EZ compared to traditional static measures.

The use of PET templates instead of T1-weighted MRI in the MNI space for generating the transformation matrix allowed the results of automated AAL segmentation comparable to the T1-weighted MRI templates. In this study, we opted for an alternative approach for invasive arterial blood sampling in patients by extracting the IDIF from the ICA instead. This non-invasive method has demonstrated its robustness through a number of studies [13, 23, 24, 27, 34, 35]. Furthermore, it can offer relative simplicity and appropriateness for clinical implementation especially for patients with DRE. Unfortunately, this study did not correct the partial volume effect (PVE) for the IDIF, as outlined in previously mentioned literature. Consequently, the measured activity concentration employed to generate the IDIF may potentially be underestimated due to this effect, especially in smaller vessels. This underestimation could influence the peak of the IDIF TAC and the fitting of the kinetic model, potentially leading to an overestimation of the kinetic parameters. We acknowledge this limitation in our study. Another limitation is the number of studied subjects was relatively small. Since only one patient proceeded with epilepsy surgery, the localization of epileptic foci was not uniformly confirmed through the standard outcome of seizure remission following the resection of the identified regions. Therefore, further studies with larger cohorts and follow-up data after epilepsy surgery are merited to validate the findings.

5 Conclusion

This study investigated whether kinetic modeling approach has a potential to improve FDG-PET localization of epileptic foci in DRE patients. The findings from this study demonstrated that the net metabolic flux (K_i) and phosphorylation (k_3) of ^{18}F -FDG, as investigated using 2-tissue irreversible compartment model in dFDG-PET, were concordance with suspected epileptogenic regions with K_i as the most reliable parameter for identifying EZ. The presumed kinetic parameters obtained from this study provide non-invasive indicators and complement clinical setting to define the potential epileptic foci in addition to the other clinical

information. This approach could contribute to more effective treatment options for DRE patients.

Data availability statement

The original contributions presented in the study are included in the article/[Supplementary Material](#), further inquiries can be directed to the corresponding author.

Ethics statement

The studies involving humans were approved by the Faculty of Medicine, Chulalongkorn University. The studies were conducted in accordance with the local legislation and institutional requirements. The participants provided their written informed consent to participate in this study.

Author contributions

KK contributed the concept, methods, patient data collection and analysis, kinetic modeling, and manuscript drafting. CS contributed the concept, image analysis, and manuscript editing. CL contributed the patient recruitment, EEG data analysis, and manuscript editing. SJ contributed the patient recruitment. AJ contributed the image acquisition and patient data collection. TH contributed the concept. ST contributed the concept, methods, data analysis and interpretation, and manuscript drafting. All authors contributed to the article and approved the submitted version.

Funding

This work was supported by the Thailand Research Fund, Thailand Science Research and Innovation (grant number

MRG6180141), and the Ratchadapiseksompotch Fund, Chulalongkorn University (grant number GB-A_61_006_30_02).

Acknowledgments

The authors would like to express their gratitude to epilepsy monitoring unit (EMU) team for taking care of the patients and sending patients for recruitment. We also thank to all Nuclear Medicine technologists at King Chulalongkorn Memorial Hospital, and at National Cyclotron and PET center Chulabhorn Hospital, Chulabhorn Royal Academy, for their help in patient data collection and image acquisition.

Conflict of interest

The authors declare that the research was conducted in the absence of any commercial or financial relationships that could be construed as a potential conflict of interest.

Publisher's note

All claims expressed in this article are solely those of the authors and do not necessarily represent those of their affiliated organizations, or those of the publisher, the editors and the reviewers. Any product that may be evaluated in this article, or claim that may be made by its manufacturer, is not guaranteed or endorsed by the publisher.

Supplementary material

The Supplementary Material for this article can be found online at: <https://www.frontiersin.org/articles/10.3389/fphy.2023.1233059/full#supplementary-material>

References

- Kwan P, Brodie MJ. Early identification of refractory epilepsy. *New Engl J Med* (2000) 342:314–9. doi:10.1056/NEJM200002033420503
- Kim S, Mountz JM. SPECT imaging of epilepsy: an overview and comparison with F-18 FDG PET. *Int J Mol Imaging* (2011) 2011:e1–e9. doi:10.1155/2011/813028
- Nasrallah I, Dubroff J. An overview of PET neuroimaging. *Semin Nucl Med* (2013) 43:449–61. doi:10.1053/j.semnuclmed.2013.06.003
- Tepmongkol S, Sriyivilaikul T, Vasavid P. Factors affecting bilateral temporal lobe hypometabolism on ¹⁸F-FDG PET brain scan in unilateral medial temporal lobe epilepsy. *Epilepsy Behav* (2013) 29:386–9. doi:10.1016/j.yebeh.2013.08.017
- Sarikaya I. PET studies in epilepsy. *Am J Nucl Med Mol Imaging* (2015) 5:416–30.
- Alabart NB, Parego XS. Imaging in epilepsy: functional studies. *Radiologia* (2012) 54:124–36. doi:10.1016/j.rxeng.2012.06.002
- Naviaux RK, Nguyen KV. POLG mutations associated with Alpers' syndrome and mitochondrial DNA depletion. *Ann Neurol Official J Am Neurol Assoc Child Neurol Soc* (2004) 55:706–12. doi:10.1002/ana.20079
- Shoffner JM, Lott MT, Lezza AM, Seibel P, Ballinger SW, Wallace DC. Myoclonic epilepsy and ragged-red fiber disease (MERRF) is associated with a mitochondrial DNA tRNA^{Lys} mutation. *Cell* (1990) 61:931–7. doi:10.1016/0092-8674(90)90059-n
- Zsurka G, Hampel K, Nelson I, Jardel C, Mirandola S, Sassen R, et al. Severe epilepsy as the major symptom of new mutations in the mitochondrial tRNA^{Phe} gene. *Neurology* (2010) 74:507–12. doi:10.1212/WNL.0b013e3181cef7ab
- Kunz WS, Kudin AP, Vielhaber S, Blümcke I, Züschratter W, Schramm J, et al. Mitochondrial complex I deficiency in the epileptic focus of patients with temporal lobe epilepsy. *Ann Neurol* (2000) 48:766–73. doi:10.1002/1531-8249(200011)48:5<766::aid-ana10>3.0.co;2-m
- Meldrum BS. Excitotoxicity and selective neuronal loss in epilepsy. *Brain Pathol* (1993) 3:405–12. doi:10.1111/j.1750-3639.1993.tb00768.x
- Seshadri V, Zarroli KA, Schetlick RS, Massey JC, Reyes JM, Eluvathingal Muttikal TJ, et al. Dynamic FDG-PET in localization of focal epilepsy: A pilot study. *Epilepsy Behav* (2021) 122:108204. doi:10.1016/j.yebeh.2021.108204
- Tang Y, Liow J-S, Zhang Z, Li J, Long T, Li Y, et al. The evaluation of dynamic FDG-PET for detecting epileptic foci and analyzing reduced glucose phosphorylation in refractory epilepsy. *Front Neurosci* (2019) 12:993. doi:10.3389/fnins.2018.00993
- Buratachwatanasiri W, Chantadisai M, Onwanna J, Chongpison Y, Rakvongthai Y, Khamwan K. Pharmacokinetic modeling of ¹⁸F-FDOPA PET in the human brain for early Parkinson's disease. *Mol Imaging Radionuclide Ther* (2021) 30:69–78. doi:10.4274/mirt.galenos.2021.08831
- Khamwan K, Plyku D, O'Reilly SE, Goodkind A, Cao X, Fahey FH, et al. Pharmacokinetic modeling of [¹⁸F] fluorodeoxyglucose (FDG) for premature infants, and newborns through 5-year-olds. *EJNMMI Res* (2016) 6:28–11. doi:10.1186/s13550-016-0179-6
- Sgouros G, Frey EC, Bolch WE, Wayson MB, Abadia AF, Treves ST. An approach for balancing diagnostic image quality with cancer risk: application to pediatric

- diagnostic imaging of ^{99m}Tc -dimercaptosuccinic acid. *J Nucl Med* (2011) 52:1923–9. doi:10.2967/jnumed.111.092221
17. Eberlein U, Bröer JH, Vandevoorde C, Santos P, Bardiès M, Bacher K, et al. Biokinetics and dosimetry of commonly used radiopharmaceuticals in diagnostic nuclear medicine—a review. *Eur J Nucl Med Mol Imaging* (2011) 38:2269–81. doi:10.1007/s00259-011-1904-z
18. Huang SC, Phelps ME, Hoffman EJ, Sideris K, Selin CJ, Kuhl DE. Noninvasive determination of local cerebral metabolic rate of glucose in man. *Am J Physiology-Endocrinology Metab* (1980) 238:E69–E82. doi:10.1152/ajpendo.1980.238.1.E69
19. Loessner A, Alavi A, Lewandrowski KU, Mozley D, Souder E, Gur R. Regional cerebral function determined by FDG-PET in healthy volunteers: normal patterns and changes with age. *J Nucl Med* (1995) 36:1141–9.
20. Löscher W. Critical review of current animal models of seizures and epilepsy used in the discovery and development of new antiepileptic drugs. *Seizure* (2011) 20:359–68. doi:10.1016/j.seizure.2011.01.003
21. Mirrione MM, Tsirka SE. Neuroimaging in animal seizure models with ^{18}F -FDG-PET. *Epilepsy Res Treat* (2011) 2011:e1–e8. doi:10.1155/2011/369295
22. Van Bogaert P, Wikler D, Damhaut P, Szliwowski H, Goldman S. Regional changes in glucose metabolism during brain development from the age of 6 years. *Neuroimage* (1998) 8:62–8. doi:10.1006/nimg.1998.0346
23. Zanotti-Fregonara P, Liow J-S, Fujita M, Dusch E, Zoghbi SS, Luong E, et al. Image-derived input function for human brain using high resolution PET imaging with ^{11}C (R)-rolipram and ^{11}C PBR28. *PLoS One* (2011) 6:e17056. doi:10.1371/journal.pone.0017056
24. Croteau E, Lavallée É, Labbe SM, Hubert L, Pifferi F, Rousseau JA, et al. Image-derived input function in dynamic human PET/CT: methodology and validation with ^{11}C -acetate and ^{18}F -fluorothioheptadecanoic acid in muscle and ^{18}F -fluorodeoxyglucose in brain. *Eur J Nucl Med Mol Imaging* (2010) 37:1539–50. doi:10.1007/s00259-010-1443-z
25. Wang G, Nardo L, Parikh M, Abdelhafez YG, Li E, Spencer BA, et al. Total-body PET multiparametric imaging of cancer using a voxelwise strategy of compartmental modeling. *J Nucl Med* (2022) 63:1274–81. doi:10.2967/jnumed.121.262668
26. Rahmim A, Lodge MA, Karakatsanis NA, Panin VY, Zhou Y, McMillan A, et al. Dynamic whole-body PET imaging: principles, potentials and applications. *Eur J Nucl Med Mol Imaging* (2019) 46:501–18. doi:10.1007/s00259-018-4153-6
27. Fahrni G, Karakatsanis NA, Di Domenicantonio G, Garibotto V, Zaidi H. Does whole-body Patlak ^{18}F -FDG PET imaging improve lesion detectability in clinical oncology? *Eur Radiol* (2019) 29:4812–21. doi:10.1007/s00330-018-5966-1
28. Hays MT, Segall GM. A mathematical model for the distribution of fluorodeoxyglucose in humans. *J Nucl Med* (1999) 40:1358–66.
29. Tepmongkol S, Tangtrairattanakul K, Lerdlum S, Desudchit T. Comparison of brain perfusion SPECT parameters accuracy for seizure localization in extratemporal lobe epilepsy with discordant pre-surgical data. *Ann Nucl Med* (2015) 29:21–8. doi:10.1007/s12149-014-0905-y
30. Sukprakun C, Limotai C, Khamwan K, Pasawang P, Tepmongkol S. A novel method of seizure onset zone localization by serial Tc-99m ECD brain perfusion spect clearance patterns. *Brain Imaging Behav* (2022) 16:1646–56. doi:10.1007/s11682-022-00640-x
31. Vielhaber S, Von Oertzen JH, Kudin AF, Schoenfeld A, Menzel C, Biersack H, et al. Correlation of hippocampal glucose oxidation capacity and interictal FDG-PET in temporal lobe epilepsy. *Epilepsia* (2003) 44:2:193–9. doi:10.1046/j.1528-1157.2003.38102.x
32. Reutens DC, Gjedde AH, Meyer E. Regional lumped constant differences and asymmetry in fluorine-18-FDG uptake in temporal lobe epilepsy. *J Nucl Med* (1998) 39:176–80.
33. Fink G, Pawlik G, Stefan H, Pietrzyk U, Wienhard K, Heiss WD. Temporal lobe epilepsy: evidence for interictal uncoupling of blood flow and glucose metabolism in temporomesial structures. *J Neurol Sci* (1996) 137:28–34. doi:10.1016/0022-510x(95)00323-t
34. Hammers A, Panagoda P, Heckemann RA, Kelsch W, Turkheimer FE, Brooks DJ, et al. ^{11}C flumazenil PET in temporal lobe epilepsy: do we need an arterial input function or kinetic modeling? *J Cereb Blood Flow Metab* (2008) 28:207–16. doi:10.1038/sj.jcbfm.9600515
35. Bertrán M, Martínez N, Carbajal G, Fernández A, Gómez Á. An open tool for input function estimation and quantification of dynamic PET FDG brain scans. *Int J Comput Assist Radiol Surg* (2016) 11:1419–30. doi:10.1007/s11548-015-1307-x